SHORT FATIGUE CRACK BEHAVIOUR IN ISO-STRESS SPECIMENS

HOGN Youshi, LU Yonghua, ZHENG Zhemin

Institute of Mechanics, Academia Sinica, Beijing, China

Fatigue tests were made on a vibration machine using specially designed specimens to investigate the initiation and propagation features of short fatigue cracks in a weld metal. The specimens were triangular in shape so that when loaded as a cantilever beam the surface tensile stress is constant. Test results show that short fatigue cracks mainly originate from slip bands within ferrite grains. The development of short fatigue cracks is marked by a gradual increase in crack density with fatigue cycles. Coalescence of short cracks leads to crack propagation and the crack path is predominantly transgranular.

KEY WORDS *iso-stress specimen, short fatigue crack, weld metal*

In recent years, there have been many studies on the problems of short fatigue cracks of metals and alloys. In this paper, a triangular specimen was specially designed, so that when subjected to a given flexural loading as a cantilever beam the maximum surface tensile stress is a constant over a large gauge length. The experimental material is a weld metal. A cyclic loading was applied to the specimen by a vibration testing machine to investigate the initiation and propagation characteristics of short fatigue cracks. Relationship between short crack behaviour and microstructure is discussed.

1. Iso-stress specimen design

1.1 *Background*

If a uniform cantilever beam specimen is subjected to a concentrated load P , the tensile stress at surface, σ, is a function of the bending moment, M:

$$\sigma(x) = \frac{M(x)t}{2J} \qquad (1)$$

where t is the thickness of the specimen, J the moment of inertia of the specimen and $M(x) = Px$. Obviously, for a constant J , the farther away the distance from the loading end is, the larger the M and therefore the greater the σ. For an arc shaped specimen [1], the maximum surface tensile stress occurs at a certain mid-section, when subjected to a concentrated load at its tip.

When these specimens are subjected to cyclic loading, the initiation and propagation of fatigue cracks will take place in a restricted region where the maximum tensile stress prevails. Experimentally it would be nice if a specimen could be designed such that the surface stress is constant over a large area.

1.2 *Iso-stress specimen*

For a cantilever beam of rectangular cross section, we have, from Eq.(1),

$$\sigma = \frac{6M}{bt^2} = \frac{6Px}{bt^2} \qquad (2)$$

where b is the width of the specimen. Eq.(2) indicates that, for a specimen with a constant thickness t and subjected to a load P , if the ratio of x to b is kept constant, then σ remains constant. The linear relation between x and b requires that the shape of the specimen be a triangle. Based on the above
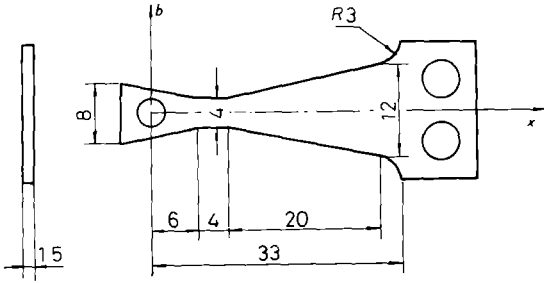
Fig. 1 Drawing of triangular shaped specimen, in mm

consideration, a triangular specimen was designed (Fig.1). In order to alleviate stress concentration and make allowance for proper loading and clamping, the ends of the specimen are modified. If the shape effect near the ends is neglected, the relation between the surface stress within the triangular section and the load applied is

$$\sigma = \frac{6KP}{t^2} = \frac{15\,P}{t^2} \qquad (3)$$

where we take $K = x / b = 2.5$.

If displacement control method is used in the loading process, a relation between the end deflection and the load applied is needed to relate the tensile stress with end deflection.

From the differential equation governing the deflection of a beam and assuming that the beam is perfectly triangular, we obtain

$$P = \frac{Et^3}{15\,L^2}\,y \qquad (4)$$

where L is length of the specimen. Substituting Eq.(4) into Eq.(3), we get

$$\sigma = Et y / L^2 \qquad (5)$$

where y is the deflection at the loading tip. Since the shape near the ends of the specimen does not conform exactly to a triangle as shown in Fig.1, it is expected that, for a given deflection y, the stress is higher than that predicted by Eq.(5). Therefore, Eq.(5) should contain a correction factor α:

$$\sigma = \alpha Et y / L^2 \qquad (6)$$

1.3 *Calculation an dcalibration of deflection-stress relationship*

To determine the value of α, we used both theoretical calculation and direct calibration. According to the second moment−area theorem [2]

$$y = \int_0^l \frac{M(x)}{EJ(x)}\,x\;\mathrm{d}x = \int_0^L F(x)\,\mathrm{d}x \qquad (7)$$

From the loading tip to clamped end, the specimen may be divided into four parts (Fig.1), hence,

$$y = y_1 + y_2 + y_3 + y_4 = 14.394(PL^2 / Et^3) \qquad (8)$$

where

$$y_1 = \int_0^{L_1} F_1(x)\,\mathrm{d}x = \int_0^{\frac{2}{11}L} \frac{6Px^2\,\mathrm{d}x}{Et^3(1.6b_0 - 0.2x)}$$

$$= 0.174\frac{PL^2}{Et^3}$$

$$y_2 = \int_{L_1}^{L_2} F_2(x)\,\mathrm{d}x = \int_{\frac{2}{11}L}^{\frac{10}{33}L} \frac{6Px^2\,\mathrm{d}x}{b_0 Et^3} = 0.720\frac{PL^2}{Et^3}$$

$$y_3 = \int_{L_2}^{L_3} F_3(x)\,\mathrm{d}x = \int_{\frac{10}{33}L}^{\frac{10}{11}L} \frac{30\,Px\,\mathrm{d}x}{Et^3} = 11.019\frac{PL^2}{Et^3}$$

$$y_4 = \int_{L_3}^{L} F_4(x)\,\mathrm{d}x$$

$$= \int_{\frac{10}{11}L}^{L} \frac{6Px^2\,\mathrm{d}x}{Et^3[4.5b_0 - \sqrt{2.5b_0^2 - (x - 15b_0)^2}]}$$

$$= 2.481\frac{PL^2}{Et^3}$$

where $b_0 = 2$ mm. Substituting Eq.(8) into Eq.(3), we have,

$$\sigma = 1.042 Ety / L^2 \qquad (9)$$

This result shows that the effect of the shape deviation on the stress−deflection relation is about 4% .

On the other hand, the result of load−deflection calibration of real specimen is listed as follows:

Load P(N)	0	4.9	9.8	14.7
Defle.y(mm)	0	0.127	0.260	0.389
Load P(N)	19.6	24.5	29.4	34.3
Defle.y(mm)	0.522	0.650	0.778	0.917

Using the linear regression method, we get,

$$y(\mathrm{mm}) = 0.02667 P(\mathrm{N}) \qquad (10)$$

for which, the correlation coefficient $r = 1.000$.

Combining Eq.(10), (8) and (3), and noting that $L = 33$ mm, $E = 2.06 \times 10^5$ MPa and $t = 1.42$ mm, we obtain:

$$\alpha = 1.038 \qquad (11)$$

The comparison of Eq.(9) and (11) shows that the two results obtained by different means are very close. In the present investigation, we use

$$\sigma = 1.04(Ety / L^2) \qquad (12)$$

i.e. $\alpha = 1.04$.

2. Experimental methods

The experimental material is a weld metal with the composition (wt−%) of C−0.12, Si−0.55, Mn−0.97, P−0.025, S−0.012, O−0.032, N−0.011, Fe balance. The specimen blanks, cut from a weld plate, were austenitized at 925 ° and then air cooled, which resulted in a normalized microstructure consisting of ferrite and pearlite. From observation and measurement by optical microscopy, the average percentage of pearlite is 16% and the average ferrite grain size is 22 μm. The yield stress of the weld, σ_y , measured by uniaxal tensile testing, is 310 MPa.

The triangular specimens were machined to the designed dimensions (Fig.1) by electric spark cutting. Both surfaces of the specimen were ground and polished, some of which were etched to reveal the ferrite, pearlite and grain boundaries.

A vibration testing machine was used to perform the fatigue testing. The wider end of the specimen was clamped in an appropriate manner and the other end was connected with the vibration machine *via* a pliable bar to permit the small amount of displacement in the longitudinal direction of the specimen. The maximum deflection of the specimen during the test was measured by means of a traveling microscope. For a given maximum deflection, the constant maximum surface tensile stress $\sigma_{\max}$, within the triangular section of the specimen, is given by Eq.(12). The specimens were fatigued at a frequency between 10 and 12 Hz and $\sigma_{\max}$ between 0.8 and 1.2 σ_y with stress ratio $R = -1$. The maximum loading cycle was 10^6.

Fatigue testing was interrupted at set intervals, during which the specimen was removed. It was then observed and photographed under an optical microscope using polarized illumination. After the examination, the specimen was put back on the machine and the same fatigue loading was again applied. Examinations at different intervals were mostly focused on serveral fixed but randomly chosen sites to track the initiation and development of short cracks.

3. Results and discussions

3.1 *Initiation of short fatigue cracks*

Isolated surface creases, *i.e.* slip markings were first observed on unetched specimens subjected to fatigue loading at $\sigma_{\max} = 0.9 \sigma_y$, $R = -1$ and fatigue cycles $N = 1$ — 3.000 (Fig.2a). As the fatigue cycle increased, additional new slip markings appeared and some of the previous ones were intensified and became slip steps. Further cycling induced the so−called extrusions and intrusions at the slip steps, which eventually evolved into short surface cracks (Fig.2b). Most short cracks initiated in the interior of
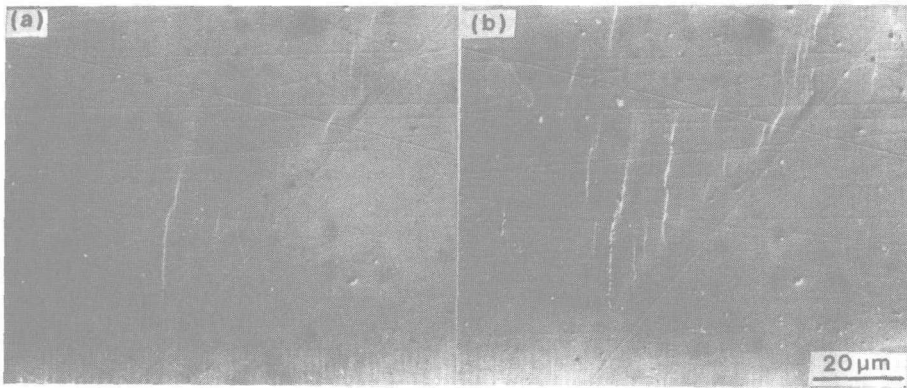
Fig. 2 Initiation of short fatigue cracks at $\sigma_{max}=0.9\sigma_y$,
transverse axis parallel to tensile stress
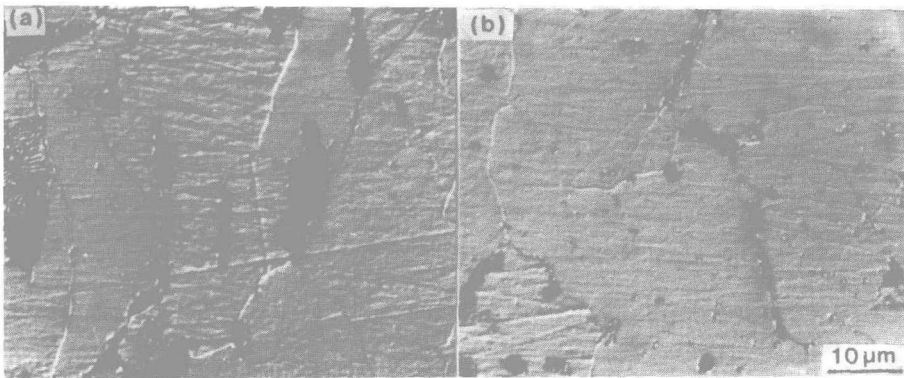(a) N=2000; (b) N=20000

Fig. 3 Short fatigue cracks after N=100 000 at $\sigma_{max}=0.9\sigma_y$,
transverse axis parallel to tensile stress
(a) inside ferrite grains; (b) close to grain boundaries

ferrite grains, although a few of them formed very close to grain boundaries, as shown in Fig.3, taken of a specimen at N = 100 000 followed by chemical etching. Since these short cracks originated from slip bands, it is understandable that they formed within the grain. For cracks appearing at grain boundaries, it is suggested that slip bands were in operation very close to the relevant grain boundaries.

Fig.4 shows the occurrence and development of short cracks from a pre-etched specimen subjected to fatigue testing at $\sigma_{max}=1.2\sigma_y$, R=-1 and N=0—127,000. A few short cracks initiated in certain ferrite

grains after only 2000 loading cycles (Fig.4b). As fatigue cycling continued, the number of short cracks gradually increased without significantly increasing the lengths of previously formed cracks. The gradual increase in the number of cracks with fatigue cycles became a typical characteristic of short crack development (Fig.4c— d). The short cracks were at least several microns in length when they appeared on the surface at this stress level. Some of them terminated with one or both ends at grain boundaries or other obstacles within the grains. The growth of these short cracks was retarded at further cycling
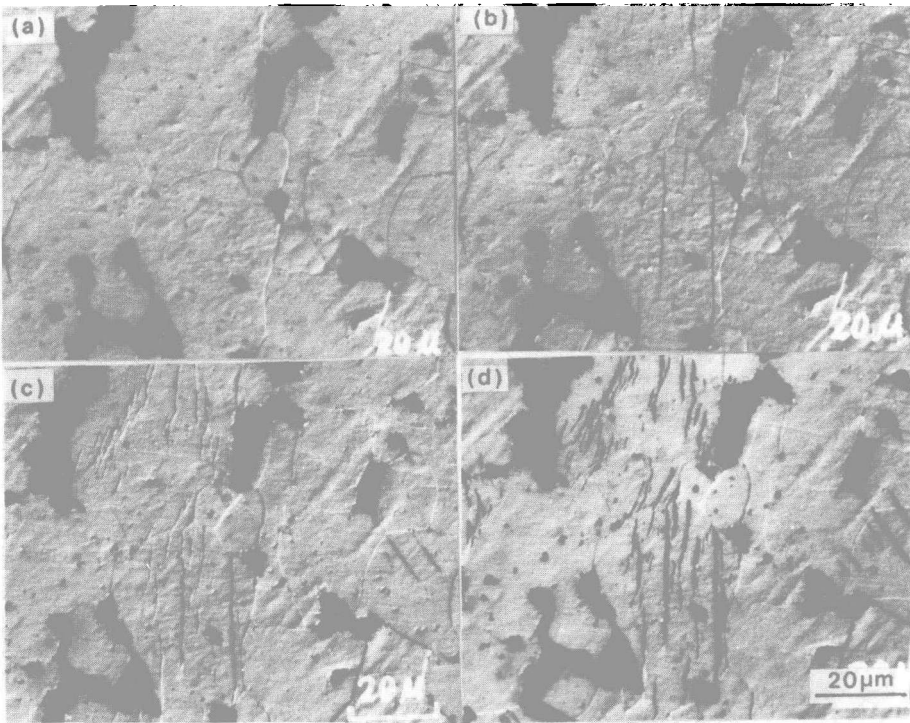
Fig. 4 Development of short cracks with fatigue cycles at
$\sigma_{max}=1.2\sigma_y$, transverse axis parallel to tensile stress
(a) $N=0$; (b) $N=2000$; (c) $N=30000$; (d) $N=127000$

(Fig.4b—d). Since grain boundaries were the main obstacles against short crack extension, in other words, the corresponding ferrite grain diameter was the maximum length for the short crack located within it, therefore, ferrite grain size was a significant microstructural factor affecting short crack behaviour.

Observations also showed that not a single short crack initiated in a pearlite domain. This is attributed to the higher strength of the pearlite, making slip more difficult to operate. Microhardness measurements showed that the value for the ferrite was 153 HV, as compared to 220 HV for the pearlite.

Macroscopically, the short cracks at initiation are usually taken to be uniform over the triangular section. Microscopically, however, they distribute quite unevenly among the different ferrite grains. This has the fol-

lowing two implications. Firstly, at the early stage, short cracks appear only in a few ferrite grains, the orientation of which tends to be nearly perpendicular to the surface tensile stress (Fig.4b). Subsequently, new short cracks initiate both in the grains containing previously formed cracks and in some others without previous cracking. The newly formed short cracks lie in directions gradually deviating from the axis perpendicular to tensile stress. The range of distribution of the angle between most short cracks and the tensile stress is between 90 and 45 ° (Fig.4c— d). Secondly, even though a specimen has been fatigued at $\sigma_{max}=1.2\sigma_y$ for more than 10^5 cycles, and short cracks have become densely distributed in many ferrite grains, a small fraction of ferrite grains remains undamaged, not a single short crack initiates in such grains (Fig.4d). It may be inferred

that, for ferrite grains where early short cracks initiate, the Schmid factor of the potential slip system is relatively larger so that this system can be easily activated; the slip system of some other grains, whose Schmid factor is somewhat lower, may be subsequently activated; and finally, the initiation of short cracks is impossible activated; and finally, the initiation of short cracks is impossible for those ferrite grains whose Schmid factor is relatively small.

3.2. *Propagation of short fatigue cracks*

As mentioned above, the development of short fatigue cracks was characterized not by the extension of the crack itself, but by the addition of new short cracks. In other words, the development of short cracks was mainly marked by the gradual increase in crack density. A few main cracks, each with a length extending over several grains, appeared when the short crack density approached a critical value. These main cracks appear to be sporadically formed mainly by the coalescence of the short cracks. Fig.5 shows such a crack that crosses several ferrite grains. The path of a main crack was predominantly transgranular. The propagation of a main crack could be caused by the
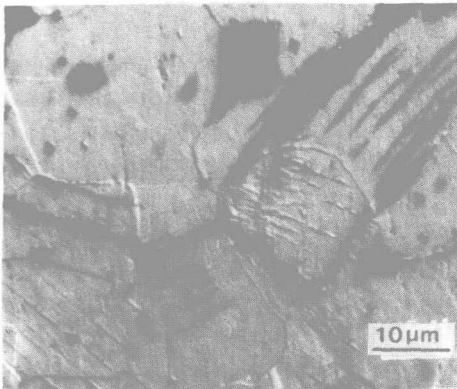
growth itself or by the coalescence with other cracks which were suitably oriented. In the present case, when most of the main cracks propagated through more than 10 grains, they coalesced, and led to the final fracture.

4. Conclusions

(1)Short fatigue cracks originate from slip bands within ferrite grains, and the length of a short crack is related to the ferrite grain size.

(2)The multiplication of short cracks is characterized by the gradual increase in crack density with fatigue cycling, and most short cracks undergo minor changes in length.

(3)The coalescence of short cracks leads to crack propagation and formation of main cracks. The coalescence of main cracks leads to the final fracture.

(4)The path of a short crack during its early propagation stage is predominantly transgranular.

(5)The triangular specimen, which provides a large specimen area at a given stress level in order to obtain more information of crack initiation and propagation, appears to be useful for investigating short fatigue crack behaviour.

Fig. 5 A main crack across several ferrite grains at $\sigma_{max}=1.2\sigma$, and $N=127000$, vertical axis parallel to tensile stress

REFERENCES

1 Gouda V K, Staehle R W. *Br Corros J*, 1980; 15 : 111—117
2 Timoshenko S P, Gere J M. *Mechanics of Materials*, New York: Van Nostrand Reinhold, 1972 : 166—217

Correspondent : HONG Youshi, Institute of Mechanics, Academia Sinica, Beijing 100080, China